

Effects of the cone-beam computed tomography protocol on the accuracy and image quality of root surface area measurements: An *in vitro* study

Chanikarn Intarasuksanti¹, Sangsom Prapayasatok², Natnicha Kampan³,
Supassara Sirabanchongkran¹, Pasuk Mahakkanukrauh^{3,4}, Thanapat Sastraruji⁵,
Pathawee Khongkhunthian⁶, Kachaphol Kuharattanachai¹, Kanich Tripuwabhrut^{1,*}

¹Department of Orthodontics and Pediatric Dentistry, Faculty of Dentistry, Chiang Mai University, Chiang Mai, Thailand

²Division of Oral and Maxillofacial Radiology, Faculty of Dentistry, Chiang Mai University, Chiang Mai, Thailand

³Department of Anatomy, Faculty of Medicine, Chiang Mai University, Chiang Mai, Thailand

⁴Excellence in Osteology Research and Training Center, Chiang Mai University, Chiang Mai, Thailand

⁵Dental Research Center, Faculty of Dentistry, Chiang Mai University, Chiang Mai, Thailand

⁶Center of Excellence for Dental Implantology, Faculty of Dentistry, Chiang Mai University, Chiang Mai, Thailand

ABSTRACT

Purpose: The objective of this study was to evaluate and compare the accuracy and image quality of root surface area (RSA) measurements obtained with various cone-beam computed tomography (CBCT) protocols, relative to the gold standard of micro-computed tomography (CT), in an *in vitro* setting.

Materials and Methods: Four dry human skulls were scanned using 8 different protocols, with voxel sizes of 0.15 mm, 0.3 mm, and 0.4 mm. Three-dimensional models of the selected teeth were constructed using CBCT and micro-CT protocols, and the RSA was automatically measured by the image-processing software. The absolute difference in the percentage of the RSA (% Δ RSA) was calculated and compared across the 8 CBCT protocols using repeated-measures analysis of variance. Finally, image quality scores of the RSA measurements were computed and reported in terms of percent distribution.

Results: No significant differences were observed in the % Δ RSA across the 8 protocols ($P > 0.05$). The deviation in % Δ RSA ranged from 1.51% to 4.30%, with an increase corresponding to voxel size. As the voxel size increased, the image quality deteriorated. This decline in quality was particularly noticeable at the apical level of the root, where the distribution of poorer scores was most concentrated.

Conclusion: Relative to CBCT protocols with voxel sizes of 0.15 mm and 0.3 mm, the protocols with a voxel size of 0.4 mm demonstrated inferior image quality at the apical levels. In spite of this, no significant discrepancies were observed in RSA measurements across the different CBCT protocols. (*Imaging Sci Dent* 2023; 53: 325-33)

KEY WORDS: Cone-Beam Computed Tomography; Dimensional Measurement Accuracy; Tooth Root; Orthodontics

Introduction

The root surface area (RSA), which is the area of the dental root that contacts the alveolar bone, is crucial in determining the appropriate force magnitude and anchorage value

for tooth movement during orthodontic treatment. Various methods have been proposed for measuring RSA. Cone-beam computed tomography (CBCT) imaging provides valuable insights into tooth structure and has been acknowledged as a suitable method for measuring RSA in both extracted and non-extracted teeth.¹⁻³ At present, CBCT is extensively utilized in dental practice to assess the hard tissue of craniofacial structures.

One of the most pressing considerations in this area is the optimization of the CBCT radiation dose. A variety of CBCT scanning parameters, including field of view (FOV),

This work was supported by the Research Fund for Postgraduate Students of the Faculty of Dentistry, Chiang Mai University, Chiang Mai, Thailand.

Received April 24, 2023; Revised August 1, 2023; Accepted August 3, 2023

Published online September 25, 2023

*Correspondence to : Prof. Kanich Tripuwabhrut

Department of Orthodontics and Pediatric Dentistry, Faculty of Dentistry, Chiang Mai University, Suthep Road, Muang, Chiang Mai 50200, Thailand
(Tel) 66-53-944464, E-mail) kanich.t@cmu.ac.th

Copyright © 2023 by Korean Academy of Oral and Maxillofacial Radiology

This is an Open Access article distributed under the terms of the Creative Commons Attribution Non-Commercial License (<http://creativecommons.org/licenses/by-nc/3.0>) which permits unrestricted non-commercial use, distribution, and reproduction in any medium, provided the original work is properly cited.

Imaging Science in Dentistry · pISSN 2233-7822 eISSN 2233-7830

voxel size, tube voltage, and tube current, influence the effective dose.^{4,5} The values of these CBCT scanning parameters should be tailored to each patient's situation and treatment plan. The aim is to adhere to the "as low as reasonably achievable"⁴ and "as low as diagnostically acceptable" principles, utilizing the minimum amount of radiation necessary to achieve adequate image quality.⁶

CBCT imaging has been employed for measurement in numerous studies, but the outcomes of both linear and volumetric measurements derived from CBCT images remain a subject of debate. A study measuring porcine tooth and root length indicated that, irrespective of voxel size (which was tested at 0.2 mm, 0.3 mm, and 0.4 mm), no significant difference was found between direct measurement using digital calipers and CBCT measurement.⁷ However, *in vitro* studies that examined volumetric tooth measurement using varying voxel sizes have reported both underestimation and overestimation of tooth volume with increasing voxel size.⁸⁻¹⁰

While the impact of voxel size on linear and volumetric tooth measurements has been explored, no research has yet been published on the effect of voxel size on RSA measurements. Furthermore, no specific CBCT protocol has been proposed for this type of measurement.¹⁻³ Consequently, the objective of this study was to compare and assess the influence of various CBCT protocols on the accuracy and image quality of RSA measurements.

Materials and Methods

This cross-sectional *in vitro* study was granted an exemption by the Research Ethics Committee (No. 7614/2020, exempted on 16/12/2020). A power analysis indicated that a minimum sample size of 32 teeth was necessary to achieve an α level of 0.05 and the desired power of 80%. This analysis was conducted using G*Power (version 3.1.9.6; University of Kiel, Kiel, Germany).

The present study involved maxillary and mandibular CBCT scans of 4 human skulls, 2 male and 2 female, as well as the micro-computed tomography (CT) scans of permanent teeth extracted from these skulls. The dry skulls were sourced from the Department of Anatomy and Forensic Osteology Research Center at the Faculty of Medicine, Chiang Mai University. From each skull, specific permanent teeth were extracted, including the right maxillary central incisors, canine, second premolar, and first molar, along with the left mandibular central incisors, canine, second premolar, and first molar. The total sample comprised 32 teeth (8 per skull).

The study incorporated dry human skulls from participants aged between 18 and 65 years, all of whom exhibited complete tooth eruption and root formation for all permanent teeth, apart from the third molar. The exclusion criteria included variation in tooth morphology, the presence of root resorptions and periapical pathology as revealed on CBCT images, the presence of dental restoration, and damage to the tooth or root incurred during extraction.

Each dry human skull was placed in a transparent acrylic container to simulate soft-tissue attenuation and was positioned on a specially designed platform that replicated the patient's positioning for each scanner. The container's position was additionally adjusted in accordance with the reference line of the unit. Eight scanning protocols, each with varying voxel sizes and FOVs appropriate for this study, were chosen from the 4 devices: 1) NewTom Giano HR (QR s.r.l., Verona, Italy), 2) Carestream Dental CS 9600 (Carestream Dental LLC, Atlanta, GA, USA), 3) DentiScan (NSTDA, Bangkok, Thailand), and 4) MobiiScan (NSTDA). The specific scanning parameters for each scanner are detailed in Table 1.

The selected teeth were carefully extracted using extraction forceps. All samples were stored in a dry container and delivered to the Research Promotion and Development unit

Table 1. Scanning parameters of cone-beam computed tomography (CBCT) protocols

Protocol	Voxel size (mm)	Field of view (cm)	Scanning time (s)	Tube current (mA)	Tube voltage (kVp)	Scan mode
NewTom Giano HR	0.15	10 × 8	26.4	4	90	Pulsed
NewTom Giano HR	0.3	10 × 8	14.4	4	90	Pulsed
Carestream Dental CS 9600	0.15	16 × 10	20	4	100	Pulsed
Carestream Dental CS 9600	0.3	16 × 10	12	3	100	Pulsed
Carestream Dental CS 9600	0.3	16 × 10	12	2	91	Pulsed
DentiScan	0.4	16 × 13	18	6	90	Pulsed
MobiiScan	0.3	16.5 × 12	12	8	90	Pulsed
MobiiScan	0.4	22 × 18.8	12	8	90	Pulsed

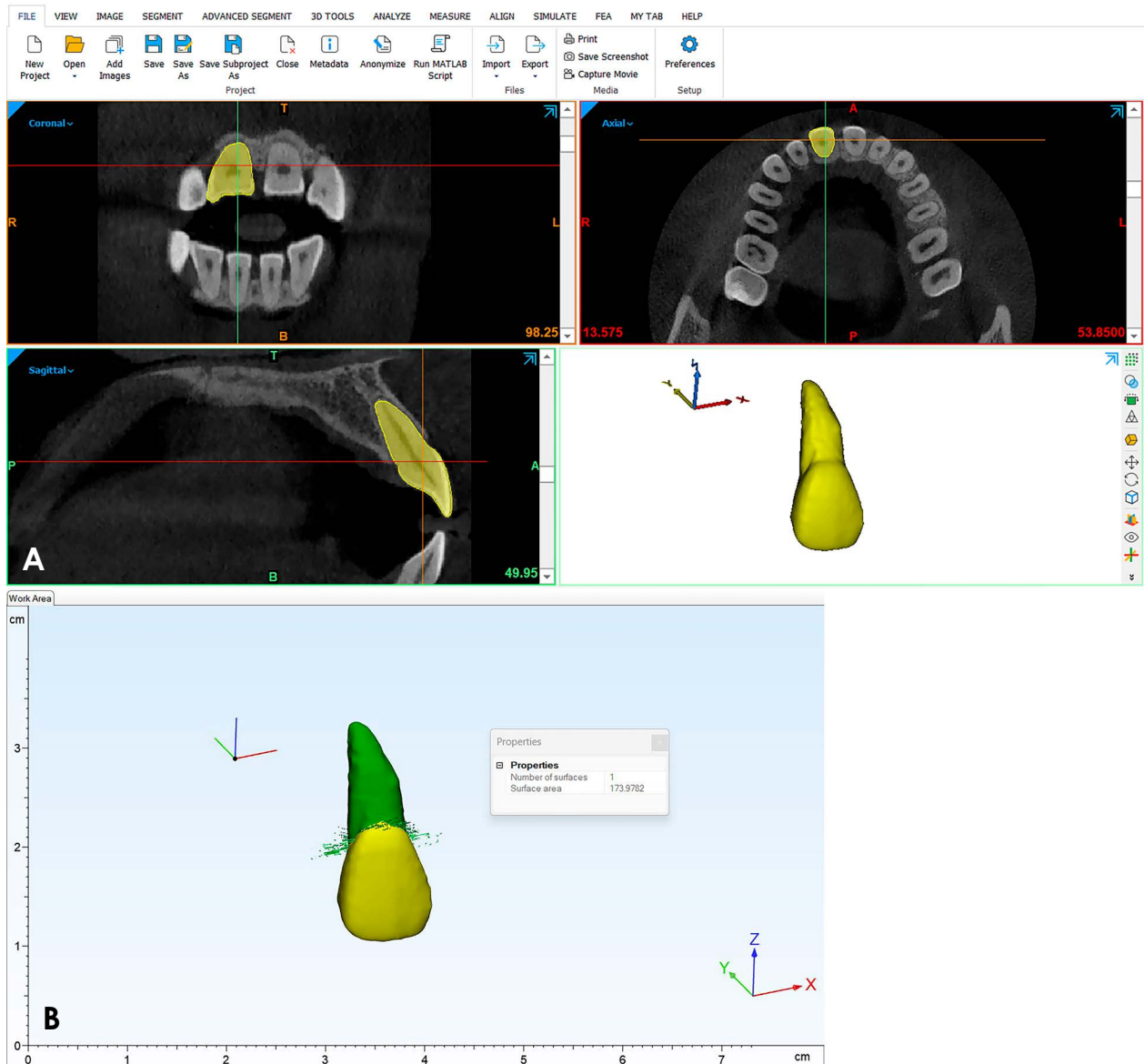


Fig. 1. A. Identification of tooth morphology on 2-dimensional images of each slice orientation and construction of a 3-dimensional tooth model. B. Identification of the cemento-enamel junction and automatic calculation of the root surface area using 3-Matic Research v. 7.01.

at the Faculty of Dentistry, Prince of Songkla University. The samples were then scanned with a μ CT 35 scanner (SCANCO Medical, Wangen-Brüttisellen, Switzerland), which served as the gold standard reference. The parameters for micro-CT scanning were set at 70 kVp, 114 μ A, and a voxel size of 18.5 μ m.

CBCT and micro-CT images were converted from Digital Imaging and Communications in Medicine (DICOM) format to stereolithography (STL) format using Mimics Research 15.01 simulation software (Materialise, Leuven, Belgium) in accordance with previously described methods.^{3,11} The resulting 3-dimensional tooth model was saved in STL

format before being imported into the 3-Matic Research 7.01 software (Materialise). The cemento-enamel junction (CEJ) was manually identified, and the RSA was automatically measured using 3-Matic Research software (Fig. 1). The operator performed the segmentation process twice, with at least a week between procedures.

The quality of images derived from all CBCT protocols was subjectively assessed for all CBCT images. This assessment was conducted by 3 observers, each with experience and published work in the use of Mimics software for tooth segmentation. The observers examined CBCT images presented as screenshots of axial slices. The distance from the

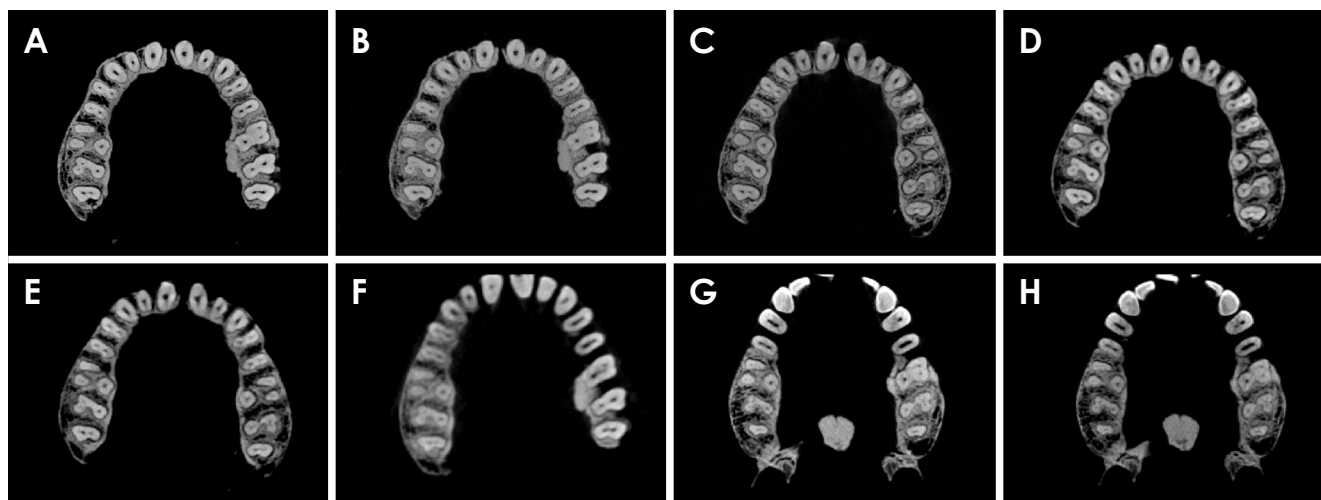


Fig. 2. Axial slice sections of the right maxillary first molar at the middle level using 8 different protocols. A. NewTom Giano HR, 0.15 mm. B. NewTom Giano HR, 0.3 mm. C. Carestream Dental CS 9600, 0.15 mm. D. Carestream Dental CS 9600, 0.3 mm. E. Carestream Dental CS 9600, 0.3 mm low-dose mode. F. DentiScan, 0.4 mm. G. MobiiScan, 0.3 mm. H. MobiiScan, 0.4 mm.

CEJ to the root apex was measured, after which the root was equally divided into 3 levels: coronal, middle, and apical. The slices from each level that offered the best visualization of the periodontal ligament space and root structure were selected for use. The observers were permitted to adjust the brightness and contrast settings. The images were displayed on a 15.6-inch ASUS Zenbook 15 (UX533) laptop monitor (ASUSTek Inc, Taipei, Taiwan), set to a screen resolution of 1920×1080 pixels. No limit was placed on observation time. The observers evaluated all images twice, with a minimum interval of 1 week between evaluations, and were blinded to the protocol used.

Image quality was evaluated based on the observer's ability to distinguish the dental root from the surrounding structures at 3 levels - coronal, middle, and apical - of the axial section (Fig. 2). The images were assessed using a 5-point rating scale. A score of 1 indicated "excellent" quality, with the entire root outline clearly identifiable. A score of 2 was considered "good," with 75% of the root outline discernible. A score of 3 was deemed "acceptable," with 50% of the root outline identifiable. A score of 4 was "bad," meaning that only 25% of the root outline could be verified. Finally, a score of 5 was "very bad," indicating that less than 25% of the root outline could be verified. A rating of "excellent" signified that the image provided a complete visualization of the root surface, enabling the entire surface to be differentiated from the surrounding structures, such as the periodontal ligament space and bone.

Statistical analysis was performed using SPSS for Windows (version 25.0; IBM Corp, Armonk, NY, USA). Mea-

surement reliability was assessed using the intraclass correlation coefficient to quantify the intraobserver and interobserver agreement. The absolute difference in the percentage of the RSA ($\% \Delta \text{RSA}$) was calculated using the formula $\% \Delta \text{RSA} = [(\text{RSA}_{\mu \text{CT}} - \text{RSA}_{\text{CBCT}}) / \text{RSA}_{\mu \text{CT}}] \times 100$. The $\% \Delta \text{RSA}$ values were then compared across CBCT reconstruction methods using repeated-measures ANOVA, with *P*-values of less than 0.05 considered to indicate statistical significance.

The overall image quality score, which indicated the observer's ability to inspect and distinguish the dental root from surrounding structures in a representative skull, was presented as a percentage distribution across the 8 protocols.

Results

The intraexaminer reliability test, conducted for the RSA measurements, demonstrated a high intraclass correlation ($r=0.998$), indicating a high degree of reliability in the measurements. Regarding image quality, the intraobserver reliability test exhibited a high intraclass correlation ($r=0.898$), while the interobserver reliability test displayed a good interclass correlation ($r=0.829$). Both of those results suggest good reliability in the image quality measurements.

RSA measurements

The Shapiro-Wilk test confirmed the normality of the RSAs, while the Levene test affirmed the equality of variances for the RSAs ($P \geq 0.05$). The absolute difference in the percentage of the RSA ($\% \Delta \text{RSA}$) was validated using

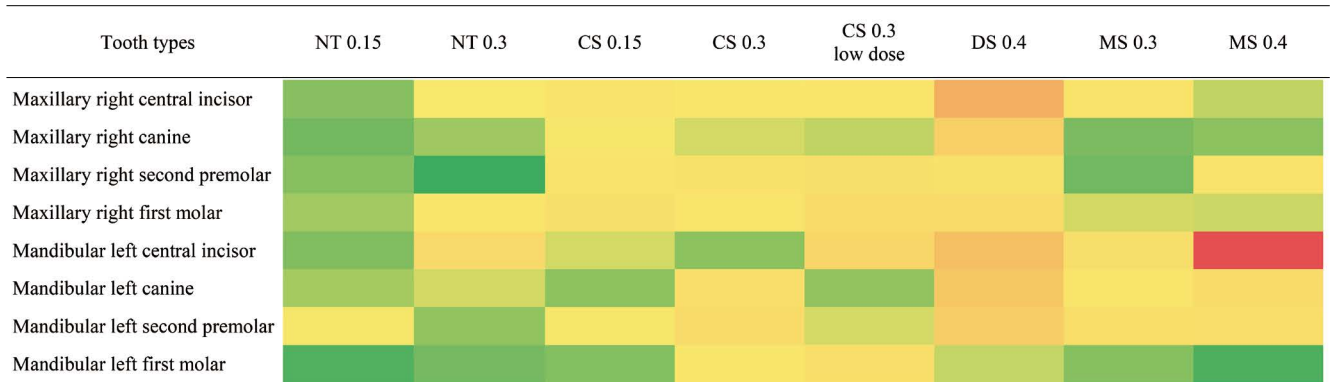


Fig. 3. Heat map of the absolute difference in the percentage of the root surface area (RSA) across the 8 protocols. The absolute difference in the percentage of the RSA was calculated as follows: $\% \Delta \text{RSA} = ((\text{RSA}_{\text{micro-CT}} - \text{RSA}_{\text{CBCT}}) / \text{RSA}_{\text{micro-CT}}) \times 100$. NT: NewTom Giano HR, CS: Carestream Dental CS 9600, DS: DentiScan, MS: MobiiScan. On the color gradient of the map, the lowest $\% \Delta \text{RSA}$ is indicated by dark green, and the highest $\% \Delta \text{RSA}$ by bright red.

Table 2. Means and standard deviations of the absolute difference in the percentage of the root surface area across tooth types and cone-beam computed tomography protocols (by ANOVA)

Tooth type	NT 0.15	NT 0.3	CS 0.15	CS 0.3	CS 0.3 low dose	DS 0.4	MS 0.3	MS 0.4	<i>P</i> -value
Maxillary right central incisor	1.42 ± 0.95	2.39 ± 0.69	2.86 ± 1.37	2.48 ± 1.70	2.70 ± 2.43	6.70 ± 2.97	2.84 ± 1.79	1.87 ± 0.48	0.111
Maxillary right canine	1.23 ± 0.97	1.61 ± 1.26	2.36 ± 1.38	2.05 ± 2.73	1.87 ± 2.18	4.39 ± 2.89	1.29 ± 0.96	1.47 ± 1.06	0.359
Maxillary right second premolar	1.41 ± 1.07	0.91 ± 0.62	2.81 ± 1.12	2.94 ± 3.03	3.15 ± 2.05	2.92 ± 2.17	1.21 ± 0.19	2.72 ± 1.52	0.382
Maxillary right first molar	1.64 ± 1.42	2.53 ± 2.64	3.11 ± 1.13	2.70 ± 1.60	3.45 ± 1.61	3.41 ± 2.95	2.03 ± 2.52	1.98 ± 1.67	0.655
Mandibular left central incisor	1.36 ± 1.90	3.60 ± 2.64	2.04 ± 0.76	1.48 ± 0.77	3.86 ± 2.42	5.61 ± 2.94	3.08 ± 1.93	13.59 ± 15.23	0.24
Mandibular left canine	1.67 ± 1.49	2.03 ± 1.87	1.47 ± 0.68	3.19 ± 1.08	1.52 ± 1.17	4.91 ± 5.78	2.64 ± 1.07	3.45 ± 1.50	0.419
Mandibular left second premolar	2.33 ± 1.80	1.51 ± 1.41	2.36 ± 1.43	3.41 ± 2.52	2.06 ± 1.46	4.54 ± 4.17	3.31 ± 2.33	3.20 ± 1.68	0.553
Mandibular left first molar	1.01 ± 0.63	1.26 ± 1.18	1.39 ± 0.89	2.58 ± 1.09	3.18 ± 0.98	1.91 ± 1.29	1.41 ± 0.82	1.01 ± 1.09	0.157

NT: NewTom Giano HR, CS: Carestream Dental CS 9600, DS: DentiScan, MS: MobiiScan

the Mauchly test of sphericity ($P \geq 0.05$). The means and standard deviations of the $\% \Delta \text{RSA}$ for each CBCT protocol are presented in Table 2. Repeated-measures analysis of variance revealed no significant differences in the $\% \Delta \text{RSA}$ across the 8 protocols ($P \geq 0.05$).

The RSA measurements derived from CBCT images exhibited deviations ranging from 1.51% to 4.30% when compared to the measurements based on micro-CT, a discrepancy that was amplified with increasing voxel size. These findings were visually represented using a heat map (Fig. 3).

Subjective image quality assessment

The image quality score, as determined by 3 observers evaluating images from the 8 CBCT protocols, was presented as a percentage distribution (Fig. 4). The images generated with a smaller voxel size were assessed to have superior image quality. The lowest image quality assessment score was attributed to the images produced with DentiScan,

using a voxel size of 0.4 mm; these were rated “acceptable.” The highest image quality across all tooth types was observed in images from the Carestream Dental CS 9600, utilizing a voxel size of 0.15 mm, which received an “excellent” rating.

Fig. 5 illustrates the percentage distribution of image quality scores across 3 root levels: coronal, middle, and apical. The apical level exhibited a greater distribution of scores deemed acceptable, bad, and very bad, followed sequentially by the middle and coronal levels.

Discussion

CBCT machines are programmed with a variety of default settings. In a clinical environment, the selection of an acquisition protocol primarily depends on the area of interest and the desired quality. The quality of the image and the process of tooth segmentation are influenced by several variables,

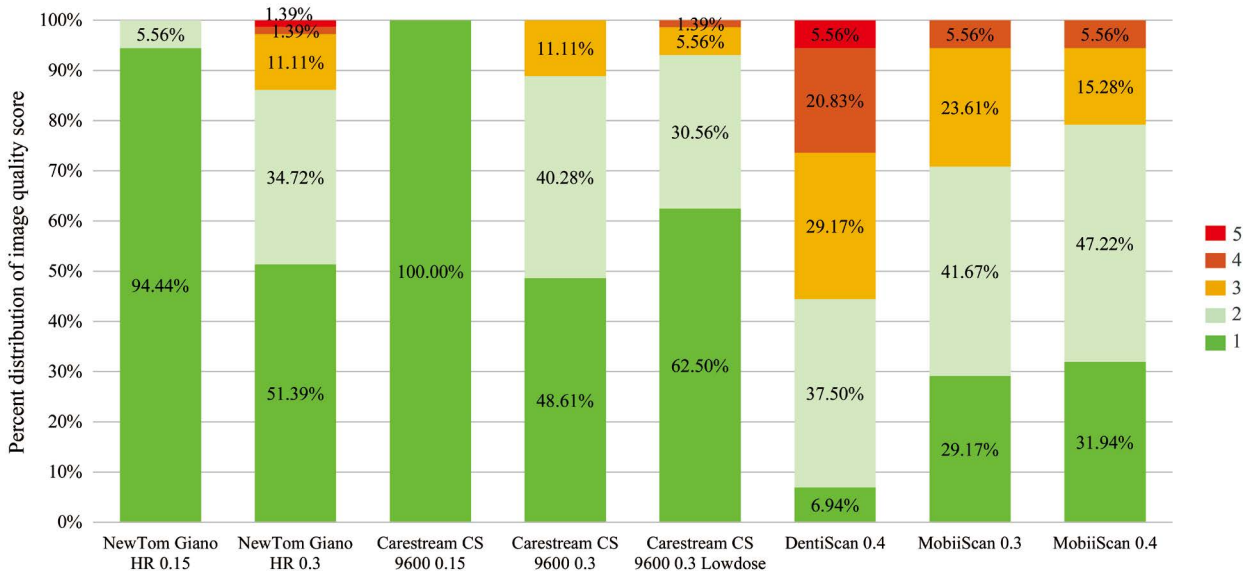


Fig. 4. Percentage distribution of the image quality score across the 8 protocols. A score of 1 was considered excellent, 2 good, 3 acceptable, 4 bad, and 5 very bad.

including CBCT parameter settings, patient-related factors, and operator-related factors.^{12,13} To control these factors as much as possible, the present study was conducted *in vitro* by a single examiner. The aim was to compare and evaluate the impact of different CBCT system factors on RSA measurement. Eight protocols were employed, primarily based on the selection of FOV and voxel size for each CBCT device. For this study, a large FOV that covered both the maxillary and mandibular teeth was chosen, and voxel sizes ranging from 0.15 to 0.4 mm were used. The type of detector, exposure time, tube voltage, tube current, rotational angle, and scan mode are all pre-set in each scanner and could not be adjusted in the chosen protocols. This study was primarily focused on voxel size and FOV, as these are the parameters most commonly adjusted in clinical situations.

The RSA refers to the portion of the dental root that contacts the surrounding periodontal tissue and bone. It plays a crucial role in determining the appropriate magnitude of force and anchorage values during the orthodontic movement of a tooth. Schwartz posits that orthodontic forces exceeding 20-26 g/cm² could potentially inflict damage on the periodontal tissue, leading to root resorption.¹⁴ The variability in RSA among patients is considered a key factor in orthodontic treatment planning.¹¹ Essentially, a tooth with a larger RSA offers better anchorage and requires a greater amount of force to induce tooth movement.¹ If the optimal force level could be determined prior to orthodontic treatment, orthodontic appliances would operate more efficiently, thereby minimizing the risk of root resorption. Moreover,

the RSA is important in providing prognoses for periodontally compromised teeth and in determining the load-bearing capacity of abutment teeth during prosthesis planning.¹⁵⁻¹⁷ Micro-CT has been extensively utilized for the evaluation of tooth structure.¹⁸ Furthermore, several *in vitro* studies have highlighted the use of micro-CT for measuring RSA, citing its high accuracy and precision in tooth measurement.^{19,20} However, this method necessitates tooth extraction, involves an extended scan duration, and generates large volumes of data that require a high-speed computer for processing.

Currently, Mimics is broadly acknowledged as the primary simulation software for utilizing segmentation and image analysis algorithms to obtain precise measurements and calculations of RSA from CBCT data.^{2,3,11,21,22} Another method for measuring RSA involves the use of algorithms developed with MATLAB (MathWorks Inc, Natick, MA, USA).¹ Essentially, the thresholding of a CBCT image is dependent on the density of the object. The density of bone structure is uniform, whereas the density of a tooth varies from the crown to the root apex. Furthermore, the contrast between the root and the surrounding structure varies across individuals and depends on the tooth's position along the jaw. A previous *in vivo* study indicated that predefined thresholding cannot be used to fully separate the teeth due to the similar densities of the tooth and surrounding bone, necessitating manual intervention. This technique can be termed semi-automatic segmentation.²³ Importantly, insufficient or excessive segmentation may result in overestima-

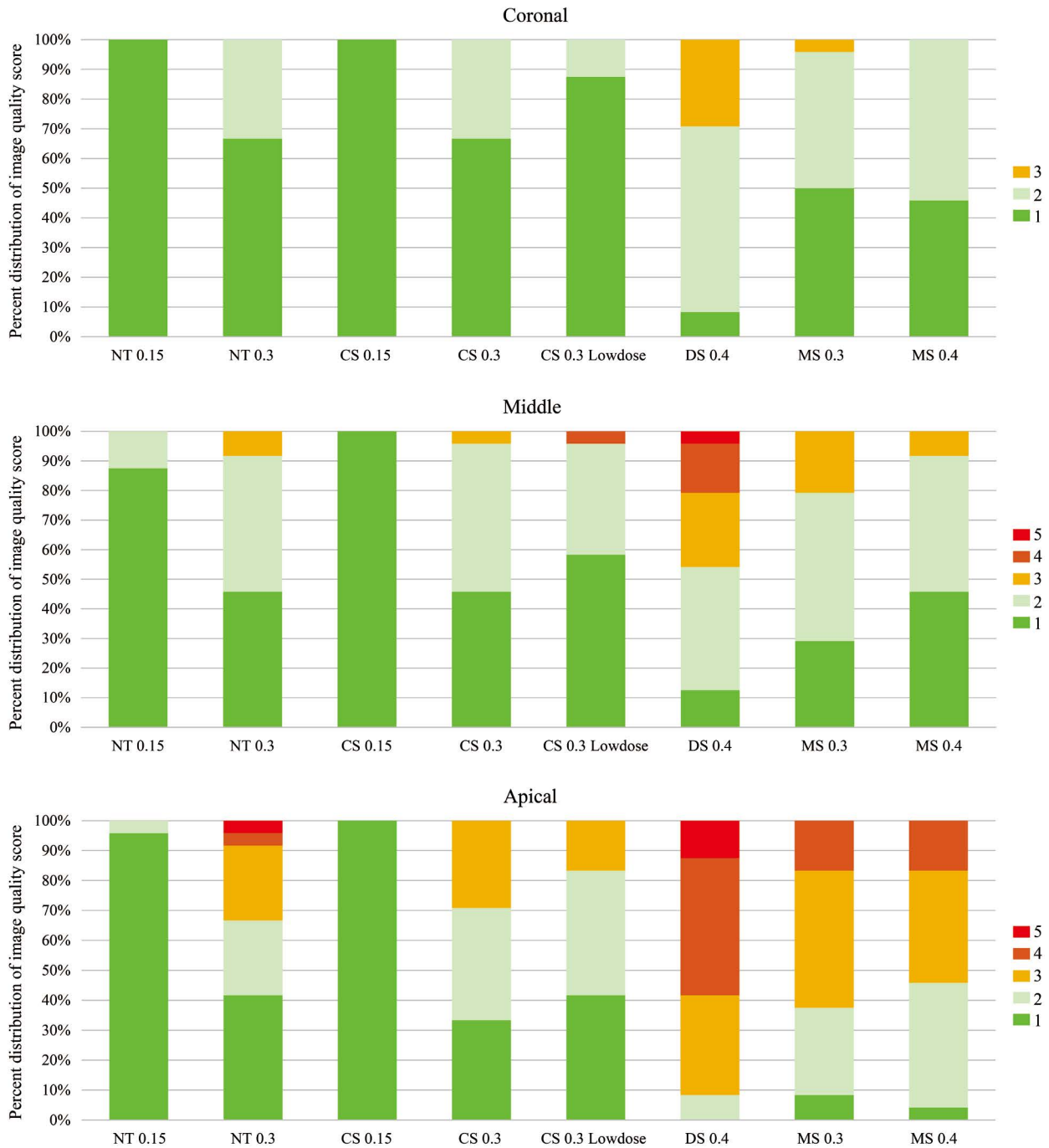


Fig. 5. Percentage distribution of the image quality score for the 3 root levels across the 8 protocols. A score of 1 was considered excellent, 2 good, 3 acceptable, 4 bad, and 5 very bad.

tion or underestimation of tooth contour, potentially leading to the miscalculation of the RSA. During the thresholding process, the present results indicated that a constant threshold value cannot be universally applied to all CBCT images obtained from different protocols. Consequently, manual and semi-automatic procedures were employed in this study, beginning with the establishment of appropriate

individual thresholding and concluding with the identification of the CEJ on the tooth model.

In this study, the findings revealed no significant disparity in the $\% \Delta \text{RSA}$ derived from all CBCT protocols, indicating accuracy in RSA measurement. Nevertheless, the deviation from the micro-CT value varied between 1.51% and 4.30%, and this deviation increased with the voxel size.

Voxel size is a defining factor of the spatial resolution of CBCT images. Certain CBCT units allow users to modify the resolution by choosing an appropriate voxel size. Although a smaller voxel size improves image resolution, it also requires a longer exposure duration, thereby increasing the radiation dose. Consequently, the optimal voxel size should be determined based on the specific purpose of the imaging.^{24,25} In particular, the voxel size should be sufficiently small to obtain satisfactory data in the area of interest. Typically, the width of the periodontal ligament varies from 0.15 to 0.38 mm; consequently, the voxel sizes selected for this study ranged from 0.15 to 0.4 mm.²⁶ Most studies of CBCT and RSA measurements have utilized a small voxel size.^{1-3,11} However, a specific protocol for RSA measurement has not yet been established.

Although the present findings did not reveal a statistical difference in the $\% \Delta \text{RSA}$ across protocols, the $\% \Delta \text{RSA}$ deviation fluctuated between 1.51% and 4.30%. The greatest deviation of the $\% \Delta \text{RSA}$ was observed in protocols involving a voxel size of 0.4 mm. This can be attributed to the fact that a larger voxel size leads to a reduced image resolution and produces more surface-surrounding artifacts.²⁷⁻²⁹ Regardless of voxel size, the smallest deviation in the $\% \Delta \text{RSA}$ was detected in the protocols from the NewTom Giano HR device. This minimal error could have been influenced by a smaller FOV.

The secondary objective of this study was to evaluate and compare the image quality scores derived from the 8 CBCT protocols. Proper image quality is crucial not only for ensuring superior diagnostic capability, but also for reducing the radiation dose in accordance with the “as low as reasonably achievable” principle. In this study, particular attention was paid to the root level, with the poorest score observed for the root’s apical region. Furthermore, 80% of the poor and extremely poor scores at this level were predominantly associated with the use of a 0.4 mm voxel size. This observation aligns with the findings of Sang et al., who reported challenges in distinguishing between the root apex and the surrounding bone due to the low contrast-to-noise ratio in CBCT.³⁰

The present findings suggest that voxel sizes between 0.15 mm and 0.4 mm are optimal for RSA measurements. While the 0.15 mm voxels yielded the smallest deviation in $\% \Delta \text{RSA}$, aligning with the best image quality score, they also required a higher radiation dose and increased the risk of patient motion artifacts due to the extended scanning time. Larger voxel sizes of 0.3 and 0.4 mm, although resulting in lower image quality, were still suitable for RSA measurements, with the $\% \Delta \text{RSA}$ deviation ranging from 1.98%

to 4.30%. However, the use of 0.3- and 0.4-mm voxel sizes may reduce the CBCT image quality, particularly at the apical levels of the tooth. Regardless of voxel size, choosing a narrower FOV could enhance both the accuracy and image quality of the RSA measurement. The insights from this study offer valuable contributions to future research and provide guidelines for the clinical application of CBCT in RSA measurements when indicated.

In conclusion, the 8 CBCT protocols used in this study exhibited optimal accuracy and image quality for RSA measurement. Although the CBCT protocols with large voxel size (0.4 mm) showed poorer image quality at the apical tooth levels for RSA measurement compared with smaller voxel sizes of 0.15 and 0.3 mm, no significant difference was observed in RSA measurement across CBCT protocols.

Conflicts of Interest: None

Acknowledgments

The authors would like to thank the Department of Anatomy, Faculty of Medicine, Chiang Mai University for its support with the human dry skull samples; Ratikorn Kittada and the staff of the Division of Oral and Maxillofacial Radiology, Faculty of Dentistry, Chiang Mai University for their helpfulness and advice regarding the CBCT acquisition technique; and the Department of Radiology, Faculty of Medicine, Siriraj Hospital, Mahidol University for its support with the simulation software.

References

1. Lakhani K, Vashishth V, Gugnani N. Root surface area measurement of permanent dentition in Indian population - CBCT analysis. *Inform Med Unlocked* 2017; 9: 1-5.
2. Park SB, An SY, Han WJ, Park JT. Three-dimensional measurement of periodontal surface area for quantifying inflammatory burden. *J Periodontal Implant Sci* 2017; 47: 154-64.
3. Tسانapanont J, Apisariyakul J, Wattanachai T, Sriwilas P, Midtbø M, Jotikasthira D. Comparison of 2 root surface area measurement methods: 3-dimensional laser scanning and cone-beam computed tomography. *Imaging Sci Dent* 2017; 47: 117-22.
4. American Dental Association Council on Scientific Affairs. The use of cone-beam computed tomography in dentistry: an advisory statement from the American Dental Association Council on Scientific Affairs. *J Am Dent Assoc* 2012; 143: 899-902.
5. Kharbanda OP, Wadhawan N, Balachandran R, Kandasamy D, Kapila SD. Functional and technical characteristics of different cone beam computed tomography units. In: Kapila SD. *Cone beam computed tomography in orthodontics: indications, insights, and innovations*. Ames: John Wiley & Sons; 2014. p. 43-66.

6. Jaju PP, Jaju SP. Cone-beam computed tomography: time to move from ALARA to ALADA. *Imaging Sci Dent* 2015; 45: 263-5.
7. Sherrard JF, Rossouw PE, Benson BW, Carrillo R, Buschang PH. Accuracy and reliability of tooth and root lengths measured on cone-beam computed tomographs. *Am J Orthod Dentofacial Orthop* 2010; 137(4 Suppl): S100-8.
8. Ye N, Jian F, Xue J, Wang S, Liao L, Huang W, et al. Accuracy of in-vitro tooth volumetric measurements from cone-beam computed tomography. *Am J Orthod Dentofacial Orthop* 2012; 142: 879-87.
9. Maret D, Telmon N, Peters OA, Lepage B, Treil J, Inglessè JM, et al. Effect of voxel size on the accuracy of 3D reconstructions with cone beam CT. *Dentomaxillofac Radiol* 2012; 41: 649-55.
10. Shaheen E, Khalil W, Ezeldeen M, Van de Castele E, Sun Y, Politis C, et al. Accuracy of segmentation of tooth structures using 3 different CBCT machines. *Oral Surg Oral Med Oral Pathol Oral Radiol* 2017; 123: 123-8.
11. Suteerapongpun P, Sirabanchongkran S, Wattanachai T, Sriwilas P, Jotikasthira D. Root surface areas of maxillary permanent teeth in anterior normal overbite and anterior open bite assessed using cone-beam computed tomography. *Imaging Sci Dent* 2017; 47: 241-6.
12. Dusseldorp JK, Stamatakis HC, Ren Y. Soft tissue coverage on the segmentation accuracy of the 3D surface-rendered model from cone-beam CT. *Clin Oral Investig* 2017; 21: 921-30.
13. Kamburoğlu K, Murat S, Kolsuz E, Kurt H, Yüksel S, Paksoy C. Comparative assessment of subjective image quality of cross-sectional cone-beam computed tomography scans. *J Oral Sci* 2011; 53: 501-8.
14. Brezniak N, Wasserstein A. Root resorption after orthodontic treatment: Part 2. Literature review. *Am J Orthod Dentofacial Orthop* 1993; 103: 138-46.
15. Gher ME, Vernino AR. Root morphology - clinical significance in pathogenesis and treatment of periodontal disease. *J Am Dent Assoc* 1980; 101: 627-33.
16. Luthra SP, Narayan I, Subrahmanyam N. Root surface area measured by the benzene adsorption method. *J Prosthet Dent* 1974; 31: 185-9.
17. Yamamoto T, Kinoshita Y, Tsuneishi M, Takizawa H, Umemura O, Watanabe T. Estimation of the remaining periodontal ligament from attachment-level measurements. *J Clin Periodontol* 2006; 33: 221-5.
18. Kim I, Paik KS, Lee SP. Quantitative evaluation of the accuracy of micro-computed tomography in tooth measurement. *Clin Anat* 2007; 20: 27-34.
19. Gu Y, Tang Y, Zhu Q, Feng X. Measurement of root surface area of permanent teeth with root variations in a Chinese population - a micro-CT analysis. *Arch Oral Biol* 2016; 63: 75-81.
20. Maret D, Molinier F, Braga J, Peters OA, Telmon N, Treil J, et al. Accuracy of 3D reconstructions based on cone beam computed tomography. *J Dent Res* 2010; 89: 1465-9.
21. Wang T, Pei X, Luo F, Jia L, Qin H, Cheng X, et al. Evaluation of tooth root surface area using a three-dimensional scanning technique and cone beam computed tomographic reconstruction in vitro. *Arch Oral Biol* 2017; 84: 13-8.
22. Jia P, Yang G, Hu W, Chung KH, Zhao Y, Liu M, et al. Comparison of in situ cone beam computed tomography scan data with ex vivo optical scan data in the measurement of root surface area. *Oral Surg Oral Med Oral Pathol Oral Radiol* 2019; 128: 552-7.
23. Wang Y, He S, Yu L, Li J, Chen S. Accuracy of volumetric measurement of teeth in vivo based on cone beam computer tomography. *Orthod Craniofac Res* 2011; 14: 206-12.
24. Spin-Neto R, Gotfredsen E, Wenzel A. Impact of voxel size variation on CBCT-based diagnostic outcome in dentistry: a systematic review. *J Digit Imaging* 2013; 26: 813-20.
25. Vizzotto MB, Silveira PF, Arús NA, Montagner F, Gomes BP, da Silveira HE. CBCT for the assessment of second mesiobuccal (MB2) canals in maxillary molar teeth: effect of voxel size and presence of root filling. *Int Endod J* 2013; 46: 870-6.
26. Nanci A, Bosshardt DD. Structure of periodontal tissues in health and disease. *Periodontol* 2000 2006; 40: 11-28.
27. Kiljunen T, Kaasalainen T, Suomalainen A, Kortensniemi M. Dental cone beam CT: a review. *Phys Med* 2015; 31: 844-60.
28. Librizzi ZT, Tadinada AS, Valiyaparambil JV, Lurie AG, Mallya SM. Cone-beam computed tomography to detect erosions of the temporomandibular joint: effect of field of view and voxel size on diagnostic efficacy and effective dose. *Am J Orthod Dentofacial Orthop* 2011; 140: e25-30.
29. Dong T, Xia L, Cai C, Yuan L, Ye N, Fang B. Accuracy of in vitro mandibular volumetric measurements from CBCT of different voxel sizes with different segmentation threshold settings. *BMC Oral Health* 2019; 19: 206.
30. Sang YH, Hu HC, Lu SH, Wu YW, Li WR, Tang ZH, et al. Accuracy assessment of three-dimensional surface reconstructions of in vivo teeth from cone-beam computed tomography. *Chin Med J (Engl)* 2016; 129: 1464-70.